ELSEVIER

Brain Research Protocols 5 (2000) 57–66

BRAIN RESEARCH PROTOCOLS

www.elsevier.com/locate/bres

Protocol

Using event-related fMRI to assess delay-period activity during performance of spatial and nonspatial working memory tasks

Bradley R. Postle *, Eric Zarahn, Mark D'Esposito

Department of Neurology, University of Pennsylvania Medical Center, 3 West Gates, Area 9, 3400 Spruce St., Philadelphia PA, 19104, USA

Accepted 8 September 1999

Abstract

Event-related experimental design and analysis techniques for functional magnetic resonance imaging (fMRI) take advantage of the intrinsic temporal resolution of fMRI to permit investigation of complex human behaviors on the time scale over which they can occur. The protocol described in this report permits the effective isolation and assessment of variance in the fMRI signal that is attributable solely to the delay portion of delayed-response tasks. It permits, therefore, evaluation of the purely mnemonic portions of working memory tasks without requiring the ''cognitive subtraction'' of nonmnemonic components of such tasks, such as visual processing and motor output. Features of this event-related fMRI technique include the empirical derivation of an impulse response function (IRF) from each subject participating in the experiment, single-subject and random effects group analyses, use of *t*-values of dependent measures, and the use of regions of interest (ROI) to improve the sensitivity of a priori contrasts. This report provides a detailed exposition of the research methodology of our event-related fMRI technique, the rationale behind many of its critical features, and examples of its application to two empirical datasets

Theme: Neural Basis of Behavior

Topic: Cognition

Keywords: Neuroimaging; Human; Caudate; Nucleus

1. Type of research

Functional magnetic resonance imaging (fMRI) offers to cognitive neuroscientists the potential to explore the neurophysiological correlates of complex human behaviors at a greater level of spatial resolution than that offered by any other currently available noninvasive neuroimaging technique. Until very recently, however, fMRI research protocols have been of the ''blocked'' variety, and have examined neural activity changes on the order of tens of seconds (for a review and discussion, see Ref. [2]). This time scale is decidedly inappropriate for the selective investigation of the neural substrates of cognitive processes that occur within seconds or milliseconds of others. Because the intrinsic temporal resolution of the fMRI signal is on the order of seconds, and not tens of seconds, the method offers the potential of designing experiments with temporal resolution superior to the limits traditionally imposed by blocked designs.

We have employed a recently developed, event-related approach to fMRI experimental design and data analysis to test hypotheses regarding the activity of the caudate nucleus associated with the performance two separate spatial and nonspatial delayed-response paradigms [17]. Each of the two paradigms has two trial types, which exemplifies the utility of event-related fMRI for testing selectivity of neural responses to different conditions. The first paradigm features ''what''-then-''where'' and ''where''-then-''what'' trials which each tap sequentially both spatial and object working memory within the same trial. The second paradigm comprises conditional visuo-motor and nonspatial delayed-matching trials that engage spatial and motor working memory and nonspatial color working memory, respectively. The particular event-related approach applied to these data [27] was developed explicitly to permit

* Corresponding author. Fax: +1-215-349-5579; e-mail: postle@mail.med.upenn.edu, http://cortex.med.upenn.edu/~postle/

1385-299X/00/$ - see front matter
PII: S1385-299X(99)00053-7

assessment of variance in the fMRI signal attributable solely to the delay period of delayed-response tasks. Its application permits the effective isolation of delay-period activity from activity attributable to other components of a delayed-response task, such as perceptual analysis and encoding processes triggered by the presentation of target stimuli, and the retrieval, decision, and motor response processes prompted by the presentation of the probe stimulus. Importantly, this technique does not rely on the logic of cognitive subtraction with respect to cognitive processes preceding or following the delay period, an approach that can lead to errors of inference [13,27,28].

This article is written with two goals in mind: (1) providing a detailed exposition of our research methodology; and (2) explaining the rationale behind many of the critical features of our event-related method. This latter goal seems particularly topical in view rapid developments of new methods for analyzing fMRI data, particularly methods that fall under the rubric of ''event-related fMRI''. Critical assessment of data produced by these new methods, a skill that is important for many neuroscientists and psychologists, increasingly requires specialized knowledge of areas of signal processing and statistics that cannot be reviewed satisfactorily in the neuroscience and psychology journals that publish these data. Our hope is that some of the descriptions of specific steps of our protocol will be better understood if they are preceded with brief treatments of the conceptual factors that motivated these steps.

2. Time required

Data collection for each subject participating in Experiment 1 of Ref. [17] proceeded in three steps: (i) T1-weighted structural MR images in 21 axial slices (spin echo pulse sequence; $0.9375 \times 0.9375 \times 5$ mm slice resolution) in an initial scan of 3 min 30 s; (ii) acquisition of blood oxygen level-dependent (BOLD)-sensitive T2*-weighted fMRI data in a preliminary scan of 5 min 40 s whose purpose was to derive an impulse response function (IRF; see Section 5.3.1; gradient echo pulse sequence; TR = 2; 160 images; $3.75 \times 3.75 \times 5$ mm slice resolution); and (iii) acquisition of BOLD data corresponding to the experimental task in eight runs of 6 min 40 s each (gradient echo pulse sequence; TR = 2; 192 images; $3.75 \times 3.75 \times 5$ mm slice resolution). Each scan began with 20 s of dummy gradient and RF pulses to achieve steady state tissue magnetization. Between structural image acquisition and the BOLD-sensitive scans, 5-10 min were required to set up and focus the visual projection equipment. Thus, one experiment required approximately 1 h 20 min. Post-processing of the data, which is detailed in Section 5 required approximately 24 h. Experiment 2 in Ref. [17] featured the same T1-weighted and IRF-derivation scanning protocols, a slightly longer scan length for the eight scans of the experimental task (gradient echo pulse sequence; TR = 2; 196 images; $3.75 \times 3.75 \times 5$ mm slice resolution), and the same post-processing procedures. Thus the time requirements for Experiment 2 were comparable to those for Experiment 1.

3. Materials

fMRI data were acquired on a 1.5 T SIGNA scanner (GE Medical Systems) equipped with a prototype fast gradient system for echo-planar imaging. A standard radio frequency (RF) head coil was used with foam padding to restrict comfortably head motion. Post-processing was performed on Sun Ultra workstations with an analysis package developed in our laboratory that features routines written in Interactive Data Language {IDL} and C. (A manual describing this analysis package in detail can be downloaded from the world wide web by visiting **http://cortex.mail.upenn.edu** and following links to ''voxbo'').

4. Policy Issues

This report conforms to the Guidelines for Responsible Conduct Regarding Scientific Communication issued by the Society for Neuroscience.

5. Detailed procedure

5.1. Subjects

We studied six right-handed subjects (five males; mean age = 23 years) in Experiment 1, and six right-handed subjects (three males; mean age = 22.7 years) in Experiment 2. All subjects were recruited from the undergraduate and medical campuses of the University of Pennsylvania, and all gave informed consent.

5.2. Behavioral procedure

5.2.1. Experiment 1: ''what''-then-''where'' and ''where''-then-''what'' trials

Experiment 1 of Ref. [17] employed a ''what''-then-''where'' delayed-response task that featured two distinct delay periods (modeled after Ref. [21], also employed in Ref. [18]). Each trial began with an instructional cue (500 ms), followed by an initial target stimulus presentation (1 s), followed by a delay period (''delay 1''; 6.5 s), followed by the simultaneous presentation of the initial target stimulus (''match'') and a foil stimulus (''intermediate stimulus presentation''; 1.5 s), followed by a second delay period (''delay 2''; 6.5 s), followed by a probe stimulus (''final probe''; 1 s; Fig. 1A). A fixation cross appeared with the

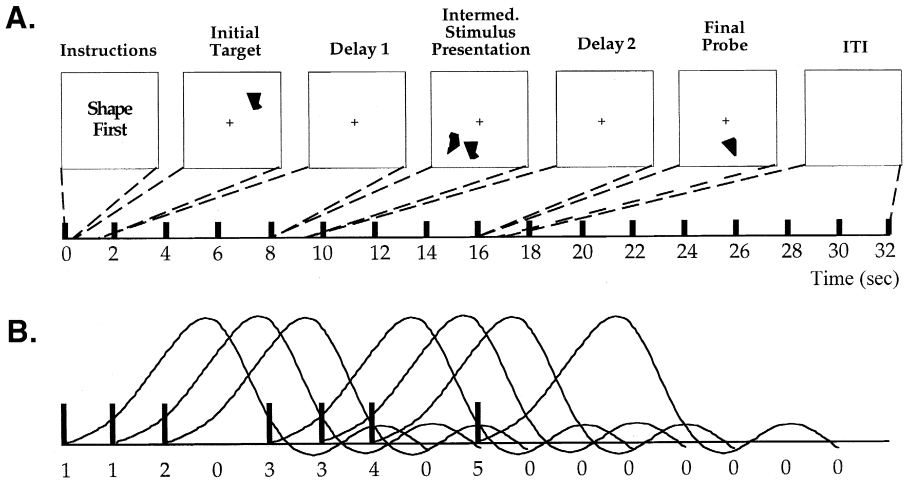

Fig. 1. (A) A schematic diagram of the components of a what-then-where trial [17,18] and a corresponding timeline. Each box represents a stimulus display event, and the dotted lines connecting each box to the timeline indicate the duration of each of these events and their position with respect to the collection of fMRI images. Ticks along the timeline represent time points in the fMRI time series. (B) Illustration of the positioning of covariates of interest employed to model variance in the BOLD signal during what-then-where trials. Vertical bars represent positioning of covariates of interest in the reference function prior to convolution with an IRF; waveforms represent these same covariates once they have been convolved with the IRF. The numbers along the timeline indicate the code assigned to each time point in the reference function that is used for data analysis.

onset of the initial target, and remained on the screen until the offset of the final probe. An intertrial interval (ITI) of 15 s separated each trial; the time from trial onset to trial onset was therefore 32 s. The instructional cue read ''shape first'' or ''location first'' in a pseudorandomly determined order. In ''shape first'' (''what''-then-''where'') trials subjects encoded the featural details of the initial target, ignoring its location on the screen, and retained this featural information during delay 1. The two intermediate stimuli both appeared in a location different from that occupied by the initial target, and their onset prompted a discrimination as to which of the two was an identical featural match with the initial target. Immediately upon making this discrimination, subjects encoded the location of the match stimulus and retained this location information during delay 2. (In this way, the match probe for the ''what'' portion of the trial became the target for the ''where'' portion of the trial). Finally, subjects indicated whether or not the final probe occupied the same location as the location target stimulus (i.e., as the match stimulus from the intermediate stimulus presentation), and indicated their decision with a ''yes'' or ''no'' button press (right or left thumb, respectively). In ''location first,'' (''where''-then-''what'') trials subjects were trained to perform spatial delayed response during the first half of the trial, and to encode featural information about the location match stimulus from the intermediate stimulus presentation in order to perform object delayed response during the second half of the trial. Each block of trials, corresponding to one fMRI experimental run, contained six ''what''-then-''where'' and six ''where''-then-''what'' trials presented in a pseudorandomized order, with an equal number of ''yes'' and ''no'' final probes for each trial type. Five of the six subjects were scanned during eight blocks of testing, and therefore each performed 48 ''what''-then-''where'' and 48 ''where''-then-''what'' trials (one subject was scanned for five blocks).

5.2.2. Experiment 2: conditional visuo-motor and nonspatial delayed-matching trials

Experiment 2 of Ref. [17] featured two tasks that were modified from Ref. [19], a conditional visuo-motor task and a nonspatial delayed-matching task that each featured color-behavior associations that subjects learned prior to scanning. In the conditional visuo-motor task, the initial presentation of either of two colored stimuli (''cue''; 600 ms) in the top position of a three-circle array indicated whether the position to choose at the end of the trial was on the left (blue cue) or the right (yellow cue). After the 11.4-s delay, the three circle array was re-presented, but with all three circles colored white (''probe''; 1 s). Subjects chose the circle on the left or the right with a button press. Cue presentation in this task informed subjects explicitly about the correct response for that trial, and thus subjects could guide performance by retaining a representation of either the spatial location associated with the cue or the motor response associated with the cue during the delay period (a prospective memory code [20,23]).

The initial cue in the delayed-matching task was red or green. Subjects remembered this color until the probe presented the two colors, in pseudorandomly determined order, in the two bottom positions, whereupon they chose the color that matched the cue. Timing, sequence, and layout of this task were identical to the conditional visuo-motor task. In contrast to the conditional visuo-motor task, however, the delayed-matching task required memory for

the color of the initial cue, and task-relevant spatial and motor information was unavailable until a response was prompted by the re-presentation of the cued color at the end of the trial. Previous behavioral testing with this task has indicated that subjects respond more quickly on conditional visuo-motor than on delayed-matching trials, consistent with the assumption that conditional visuo-motor trials permit motor preparation during the delay period [6].

5.3. fMRI data processing

Our inferential statistics were derived using multiple regression. We modeled the BOLD signal changes occurring during each qualitatively distinct component of the behavioral trials (e.g., for Experiment 1, *initial target*, *delay 1*, *intermediate stimulus presentation*, *delay 2*, and *final probe*) with a series of covariates (Table 1) that were entered into a general linear model (GLM) for autocorrelated observations [25]. Each covariate comprised an IRF positioned appropriately to represent neural activity associated with one of the task components (Fig. 1B; Fig. 2A) [27]. The positioning of covariates in the design matrix of the GLM was accomplished by first constructing a reference function that represented the *onset* of neural activity correlated with each stimulus display event (i.e., for Experiment 1, *initial target*, *intermediate stimulus presentation*, and *final probe*), and the *midpoint* of each delay period (i.e., *delay 1* and *delay 2*). Next, we convolved each covariate with the empirically derived BOLD IRF for that subject (Fig. 1B; see Section 5.3.1). This step effectively transformed the reference function from a model of predicted neural activity to a model of predicted BOLD activity (Fig. 2A). Although the initial reference function representing neural activity as discrete impulses would do a poor job of modeling neural activity, these same covariates, once convolved with an IRF, are suitable for modeling BOLD signal. The 4-s spacing between these covariates was chosen to mitigate colinearity (i.e., shared variance) while ensuring that the likely set of BOLD fMRI responses would be modeled [27]. To avoid confusion with other covariates that are also entered into the GLM, the covariates discussed in this paragraph will be referred to as ''covariates of interest'' from this point forward. The covariates of interest for Experiments 1 and 2 are listed in Table 1.

The least-squares solution of the linear model of the dependent data (i.e., of the fMRI time series) yielded parameter estimates (i.e., beta values) that were associated with each covariate of interest. These parameter estimates are interpreted as indices of the extent to which their corresponding covariates of interest explain the dependent data. Statistical maps were generated by computing *t*-statistics associated with linear combinations of the covariates of interest (see Section 5.3.3).

5.3.1. IRF derivation

Research in our laboratory indicates that (i) the shape of the BOLD response to a brief impulse of neural activity (i.e., the IRF) can differ considerably from subject to subject, and (ii) the shape of the IRF for an individual subject varies very little within a scanning session [4]. (i) indicates that models of fMRI data will have greater sensitivity and validity if they employ as a convolution kernel an IRF derived from the subject whose data are being analyzed than if they use a generic smoothing kernel, such as a Gaussian or a Poisson function. (A generic smoothing kernel is, to our knowledge, employed by every research group employing a similar approach to event-related fMRI). (ii) indicates that we need not be concerned that the estimate of an IRF obtained near the beginning of an fMRI scanning session may be less valid for modeling data acquired near the end of that same session. The first step of each scan in our event-related fMRI experiments, therefore, was to derive empirically an estimate of the IRF for each subject.

During the IRF derivation scan, each subject performed a simple reaction-time task that required a bimanual button press once every 16 s in response to a change in shape of a fixation stimulus. A partial *F*-test associated with a Fourier basis covariate set [14] was used to evaluate the significance of task correlated activity in each voxel of primary somatosensory and motor cortical regions of interest [9].

Table 1
Covariates of interest in the two experiments described in Ref. [17].
For ease exposition, the parenthetic titles are used in the text.

Experiment 1: ''what''-then-''where''	Initial target$_{\text{what-then-where}}$ (''object'')	Experiment 2: ''motor set''	Target$_{\text{conditional visuo-motor}}$
	Delay 1$_{\text{what-then-where}}$ (''object'')		Delay 1$_{\text{conditional visuo-motor}}$
	Intermediate stimulus presentation$_{\text{what-then-where}}$		Delay 2$_{\text{conditional visuo-motor}}$
	Delay 2$_{\text{what-then-where}}$ (''spatial'')		Probe$_{\text{conditional visuo-motor}}$
	Final probe$_{\text{what-then-where}}$ (''spatial'')		Target$_{\text{delayed-matching}}$
	Initial target$_{\text{where-then-what}}$ (''spatial'')		Delay 1$_{\text{delayed-matching}}$
	Delay 1$_{\text{where-then-what}}$ (''spatial'')		Delay 2$_{\text{delayed-matching}}$
	Intermediate stimulus presentation$_{\text{where-then-what}}$		Probe$_{\text{delayed-matching}}$
	Delay 2$_{\text{where-then-what}}$ (''object'')		
	Final probe$_{\text{where-then-what}}$ (''object'')		

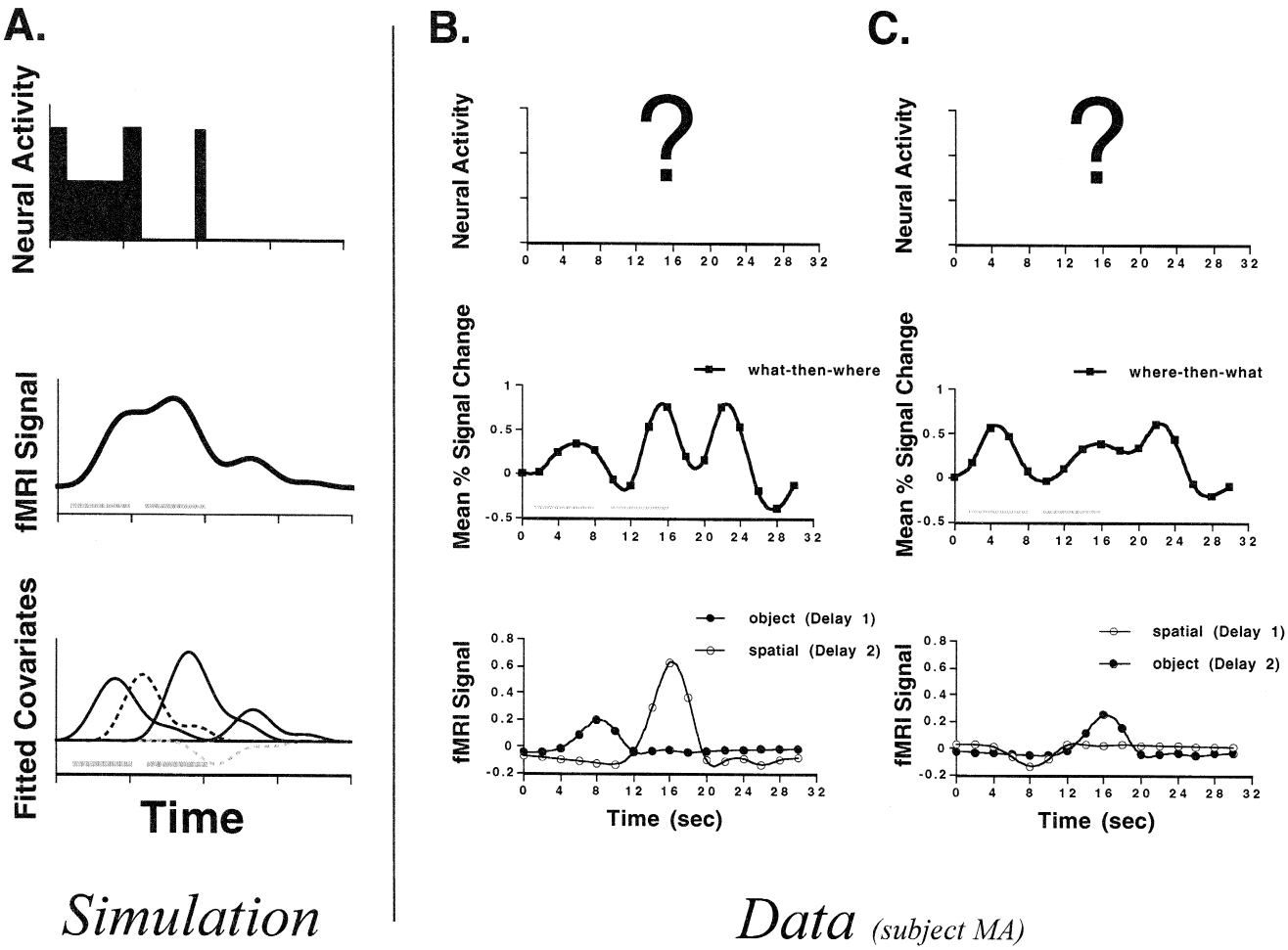

Fig. 2. (A) Top row: Simulated neural activity in a hypothetical voxel responding to *initial target*, *delay 1*, *intermediate target*, and *final probe* periods of a what-then-where task. (In this simulation, there is no neural activity during *delay 2*). The simulated resultant BOLD fMRI signal from this voxel (middle row) was generated by convolving the simulated neural activity with an empirically derived IRF. The plots in the bottom row illustrate the least-squares solution of a modified GLM, i.e., the extent to which each of the five covariates is sensitive to variance in the simulated time series. Note that the model detects significant activity attributable to *delay 1* (black dashed line), but no activity attributable to *delay 2* (gray dashed line). Gray bars represent delay periods. (B) An illustration of the implementation of event-related fMRI analysis with trial-averaged BOLD fMRI data from a single voxel in the right head of the caudate nucleus of a single subject, originally presented in Fig. 1b of Ref. [17], and re-presented in Fig. 4 of the present report. The time series in the middle row represents the activity in this voxel averaged across 48 what-then-where trials. The bottom row presents the results of the GLM, for this voxel, for the two delay-periods associated with what-then-where trials: each plot represents a covariate scaled by its parameter estimate. Visual inspection suggests that delay 2 activity was greater then delay 1 activity in what-then-where trials. (C) An illustration analogous to that presented in (B), but for where-then-what trials. Visual inspection of the results of the GLM suggest that there was a slight decrease in activity (compared to baseline) during delay 1.

(More details on region-of-interest {ROI}-based analyses are provided in Section 5.3.2.2). An IRF estimate was extracted from the suprathreshold voxels of these ROIs by spatially averaging their time series, filtering the resultant averaged fMRI time series to remove high (> 0.244 Hz) and low (< 0.05 Hz) frequencies, adjusting it to remove the effects of nuisance covariates [11], and trial averaging (see Fig. 3).

5.3.2. Hypothesis testing: rationale for both single subject and groups levels

Our analyses were performed in two steps: single subject analyses and group analyses. Single subject analyses permitted us to maintain the high spatial resolution afforded by fMRI, and to detect intersubject variability. The latter information is typically lost in analysis approaches that combine data from all subjects at an early stage of analysis, and are thus restricted to testing for activation patterns that are consistent enough across subjects in a standard space to be detected after group-averaging. Our single subject analyses, in contrast, treated each subject as a case study, and permitted us to assess replication of (as well as variation in) effects across individual cases. In essence, data from six subjects performing the same task represented a single result with five replications. Single subject analyses with methods comparable to those described here (and, importantly, with a large number of

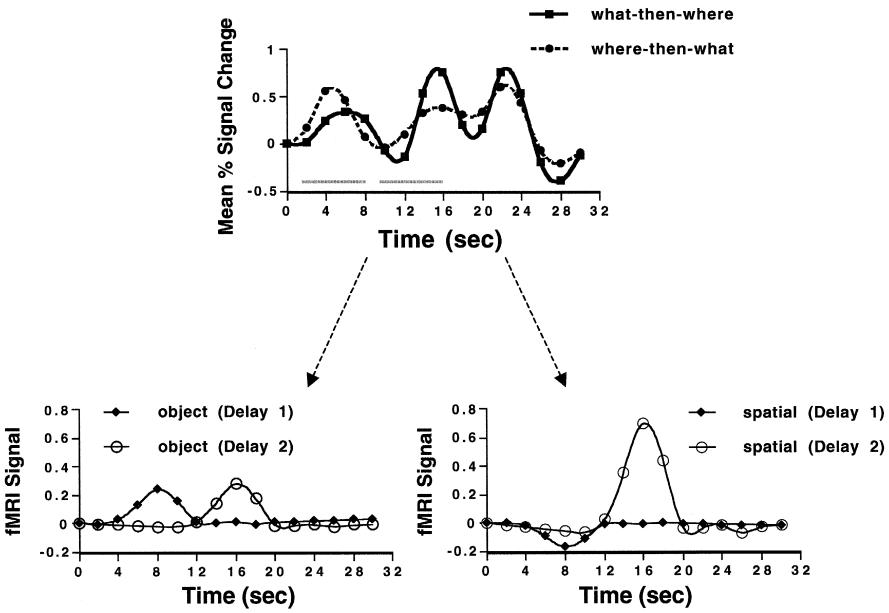

Fig. 3. The top row re-presents the trial-averaged fMRI data from Fig. 2B and C, superimposed onto the same set of axes. The charts in the bottom row re-present the plots of delay-period covariates scaled by their parameter estimates, now rearranged to illustrate schematically the values entered in the contrasts; [*object delay 1 − object delay 2*] on the left; and [*spatial delay 1 − spatial delay 2*] on the right. Visual inspection suggests that activity in this voxel was comparable during object delay 1 and object delay 2, whereas it was markedly less during spatial delay 1 than during spatial delay 2, an impression confirmed by the *t*-values resulting from these two contrasts, −0.3 and −3.8, respectively.

observations per subject, as in the present study) have been demonstrated to feature ample sensitivity to detect signal intensity changes of interest [8,28]. For example, contrasts performed with single subject data in Ref. [17] had in excess of 1200 effective degrees of freedom.

Our group analyses were performed as random effects models, which permit generalization of results obtained from a sample to the population represented by that sample. This inferential step cannot be made with the fixed effects group analyses that have been employed by the majority of fMRI experimentalists to date [12,24]. Importantly, random effects analyses are more robust to spurious results that can arise if a disproportionately large effect size in a single subject ''drives'' the mean effect size for the group, as can happen with fixed effects analyses. All our group analyses used *t*-values as dependent measures (see Section 5.3.4.1).

So, the purpose of using both single subject and group analyses were that they each provided complementary information. The single subject analyses provided information about the reliability of effects in individual subjects as well as the variability in the locations of true activation across subjects with high spatial resolution. The group analysis allowed explicit testing of population-level hypotheses (which need not be associated with statistically significant results within each subject).

5.3.2.1. Hypothesis testing: multiple comparison problem. In order to control the omnibus false positive rate, one must take into account the number of independent statistical tests performed when determining the threshold [15]. In an fMRI dataset from subject MA in Ref. [17], for example, 15,228 (approximately) independent statistical tests (one for each voxel in the brain) would be performed to generate a whole-brain statistical map. One method for correcting for multiple statistical tests, Bonferroni correction, has been demonstrated to control the false-positive rate when applied to *unsmoothed* data analyzed with the method described in this report [3,26]. Importantly, Bonferroni correction is not ''too stringent'' in general (as often claimed) when the comparisons are independent. In fact, in such cases it gives almost an exact correction for small voxel-wise false positive rates. The Bonferroni correction is applied as follows: To control the omnibus false positive rate for tests at N independent voxels at α, use the threshold that controls the voxel-wise false positive rate at α/N.

5.3.2.2. Hypothesis testing: regions of interest. All the analyses reported in Ref. [17] were performed with ROIs. This approach increased our sensitivity to detect activity in regions defined a priori, because the critical *t*-value for a contrast performed within a several hundred-voxel ROI (e.g., t of 3.6 for the 158-voxel caudate nucleus ROI of subject MA) would be lower than the critical *t*-value for the same contrast performed across the volume of the entire brain (t of 4.7 for the 15,228-voxel whole-brain dataset of subject MA).

Caudate nucleus ROIs were drawn for each subject on that subject's T1 anatomical images, and incorporated the

head of the caudate nucleus, beginning rostrally and ventrally at approximately the level of the anterior commissure, and the body of the caudate nucleus, extending caudally along the lateral wall of the lateral ventricle and ending at the ventral-most level at which the body of the lateral ventricle appeared intact in one slice (i.e., one slice dorsal to the slice in which the atrium became visible; Fig. 4). We also performed analyses on three cortical areas that are linked anatomically and functionally with the basal ganglia: areas 9 and 46 of dorsolateral prefrontal cortex (DLPFC), primary motor cortex (M1), and area 7 of posterior parietal cortex (PPC). We created ROIs for DLPFC and PPC by drawing them onto the ''canonical'' representation of a brain in Talairach space that is provided in SPM96b, using the atlas of Talairach and Tournoux [22] to confirm our identification of anatomical landmarks. Next, we transformed these ROIs from Talairach space into the native space in which each subject's data had been acquired by applying the 12 parameter affine transformation [10] with nonlinear deformations [5], routine in SPM96b (effectively, a ''reverse normalization''). We defined the M1 ROI on each subject's T1 anatomical images as the cortex immediately anterior to the central sulcus.

5.3.3. Single subject analyses

In Experiment 1, we effected tests of our first hypothesis, a main effect of stimulus material in the caudate nucleus, by generating a two-tailed *t*-map of the contrast [*(spatial delay 1 + spatial delay 2) − (object delay 1 + object delay 2)*] and detecting suprathreshold voxels. We tested our second hypothesis, effects of position in delay-period activity, by generating two-tailed *t*-maps of the contrasts [*spatial delay 1 − spatial delay 2*] and [*object delay 1 − object delay 2*]. The identification of suprathreshold *t*-values in this analysis would indicate that delay-period activity within a particular working memory condition (spatial or object) was sensitive to position within the trial. Analysis of activity during the response phase of the task [*spatial final probe − object final probe*], assessed whether the caudate nucleus displayed differential motor activity.

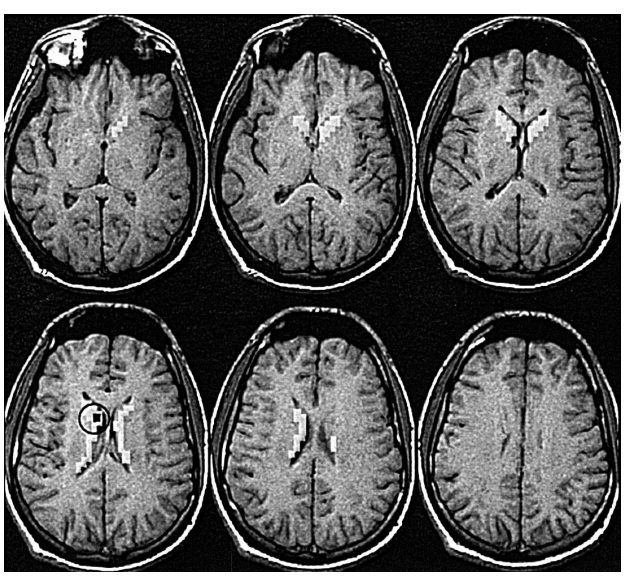

Fig. 4. Superimposed on these T-1 anatomical images from subject MA are the caudate nucleus ROI (translucent white) and the voxel that was significant for contrast [spatial delay 1 − spatial delay 2] (circled).

In Experiment 2, we tested our first hypothesis, a main effect of task, by generating a two-tailed *t*-map of the contrast [*(Conditional visuo-motor delay 1 + Conditional visuo-motor delay 2) − (Delayed-matching delay 1 + Delayed-matching delay 2)*] and detecting suprathreshold voxels. We tested our second hypothesis, effects of position in delay-period activity, by generating two-tailed *t*-maps of the contrast [*Conditional visuo-motor delay 1 − Conditional visuo-motor delay 2*] and of the contrast [*Delayed-matching delay 1 − Delayed-matching delay 2*]. The identification of suprathreshold *t*-values in this analysis would indicate that delay-period activity within a particular task was variable over time. We also tested for differential motor activity with a contrast of probe-related activity in the two tasks.

5.3.4. Group analyses

In Experiment 1, group tests for a main effect of stimulus material were performed by first identifying for each subject the voxels within the caudate nucleus ROI showing a main effect of delay period activity [*spatial delay 1 + spatial delay 2 + object delay 1 + object delay 2*] and, from these voxels, extracting a spatially averaged time course and calculating the orthogonal two-tailed contrast of [*(spatial delay 1 + spatial delay 2) − (object delay 1 + object delay 2)*]. The resultant *t*-value represented, for each subject, the extent to which the sensitivity of delay-period activity was greater for spatial or for object stimuli. (A positive *t*-value would indicate that spatial delay-period activity was greater than object delay-period activity, a negative *t*-value the converse.) This *t*-value was used as data in the subsequent group analysis [Section 5.3.4.1]. A paired *t*-test on these *t*-values, one from each subject, assessed the significance of any trends in the data across subjects. To conduct group analyses of our second hypothesized effect, a greater influence of trial position on delay-period activity with one stimulus type than with another, we generated an index of the sensitivity of caudate nucleus activity to trial position by identifying critical voxels showing a main effect of delay period activity within the caudate nucleus ROI, extracting a spatially averaged time course from these critical voxels, and calculating the orthogonal contrast of [*(spatial delay 1 − spatial delay 2) − (object delay 1 − object delay 2)*]. The two-tailed *t*-value arising from this contrast represented, for each subject, a noise-normalized measure of the interaction of stimulus material and delay period position. A paired *t*-test on these *t*-values, one from each subject, assessed the significance

at the group level of this interaction. Comparable analyses were performed within the DLPFC, M1, and PPC ROIs.

Random effects group analyses were also performed on the first hypothesis of Experiment 2 by generating a one-tailed *t*-map of the main effect of delay-period activity for each subject [*Conditional visuo-motor delay 1 + Conditional visuo-motor delay 2 + Delayed-matching delay 1 + Delayed-matching delay 2*], identifying suprathreshold voxels and extracting from them a spatially averaged time series, applying to this time series the orthogonal contrast of [*(Conditional visuo-motor delay 1 + Conditional visuo-motor delay 2) − (Delayed-matching delay 1 + Delayed-matching delay 2)*], and performing a paired *t*-test on the resultant *t*-values contributed by each subject. We tested our second hypothesis, an interaction of task and position in delay period, by extracting a spatially averaged time course from the voxels in the caudate nucleus ROI showing a main effect of delay-period activity, calculating the orthogonal contrasts of: [*(Conditional visuo-motor delay 1 − Conditional visuo-motor delay 2) − (Delayed-matching delay 1 − Delayed-matching delay 2)*], and performing a paired *t*-test on the resultant *t*-values contributed by each subject. As in Experiment 1, this analysis would be repeated in M1 to confirm the mnemonic nature of this interaction.

5.3.4.1. t-Values as dependent measures. An important consideration regarding the sensitivity of random effects group analyses is minimization of unexplained intersubject variance. Analysis of fMRI data from our laboratory have revealed that fMRI data from different scans can differ from each other by one or more scaling factors (Zarahn, E., Scaling noise in BOLD fMRI data, manuscript in preparation). [1] This is manifested as different levels of absolute fMRI signal intensity in the raw data. The scaling factor that characterizes this variance is essentially multiplicative noise that would introduce noise into random effects analyses that incorporated data from different scans, and thus decrease the power of these analyses. The signal-to-noise ratio of a random effects test on these data normalized by their residual error estimates was 2.6 times that of a test performed on the unnormalized data, and 1.5 times that of a test performed on data normalized by the time series mean (i.e., % change data; Zarahn, E., Scaling noise in BOLD fMRI data, manuscript in preparation). The implication of these results for our group analysis method is that normalization of effect sizes across subjects is more effectively accomplished via normalization by the noise factor within each subject's data, than via normalization by the mean signal intensity level. The *t*-value is such a noise-normalized index of an effect.

A common objection to the use of *t*-values as measures of effect size is quite simply that they are not in general employed as measures of signal-to-noise ratio. However, if the *t*-values are all obtained from the same contrast, from the same type of design, and from the same type of observational unit (e.g., normal human subjects) with the same magnitude of within-unit measurement error, then they indeed provide a measure of effect size that accounts for across-scan scaling factors.

6. Results

6.1. Experiment 1: Single subject analyses

The test of our first hypothesis yielded a null result: direct contrast of spatial vs. object delay-period activity (collapsed across trial position) revealed no suprathreshold voxels in the caudate nucleus in any subject. Similarly, the contrast of delay 1 vs. delay 2 (collapsed across stimulus material) yielded no significant differences in any subject. We did, however, observe effects of delay position within stimulus material in several subjects: Trial-position differences (delay 2 > delay 1) achieved significance in the caudate nucleus for four subjects in the spatial condition, as contrasted with only one subject in the nonspatial condition. Spatial delay 2 > delay 1 suprathreshold voxels were located in the right head of the caudate nucleus in two subjects, in the left head of the caudate nucleus in one subject, and bilaterally in the head of the caudate nucleus in one subject (subject EP); object delay 2 > delay 1 voxels were also found in the head of the caudate nucleus, bilaterally, in subject EP, although in a different, nonoverlapping set of voxels. Probe differences (spatial final probe > object final probe) were significant in only one subject. No significant trial-position effects were observed with delay-period activity in DLPFC, M1, or PPC.

6.2. Experiment 1: Group analyses

All group analyses failed to achieve significance in each of the four ROIs (caudate nucleus, DLPFC, M1, PPC).

6.3. Experiment 2: Single subject analyses

Analysis of delay-period activity in caudate nucleus ROIs revealed no overall effects of task (conditional visuo-motor, delayed matching) or of position in the delay (delay 1, delay 2) — a failure to reject the null hypothesis that there was no main effect of task. There was, however, a significant position effect (delay 1 > delay 2) in the conditional visuo-motor task in four of the six subjects, as contrasted with a significant position effect (delay 1 > delay 2) in two of the six subjects in the delayed-matching task. Suprathreshold voxels identified in the conditional

[1] These analyses can be viewed by visiting our laboratory's website at **http://cortex.med.upenn.edu/** and following links to ''papers'', then to ''notes'', and finally to ''Studies of gain artifacts in fMRI data''.

visuo-motor task were located in the right head of the caudate nucleus in two subjects, in the left head and left body of the caudate nucleus in one subject, and bilaterally in the head of the caudate nucleus in one subject. There were no differences in probe-related activity in any subjects. Suprathreshold voxels identified in the delayed-matching task were overlapping with, or adjacent to, the voxels identified in the conditional visuo-motor task: right head and left body in one subject, and left head and left body in one subject.

6.4. Experiment 2: Group analyses

These revealed no significant effects of task or of position in the delay. The analysis of the task by delay-position interaction in caudate nucleus, however, revealed greater sensitivity to delay position in the conditional visuo-motor task than in the delayed-matching task in each of the five subjects for whom we performed this analysis ($t(4) = 6.9$; $p < 0.005$). This effect was not observed in frontal areas 9 and 46 or M1, or in posterior parietal area 7. Finally, there was no significant difference in probe-related activity.

7. Discussion

The results of Ref. [17] indicated qualitatively different delay-period activity in the caudate nucleus during spatial than nonspatial tasks. We interpreted these results to be consistent with the view that spatial delay-period activity in the caudate nucleus features greater interaction with the motor system than does nonspatial delay-period activity [1,7]. The strongest evidence for this interpretation arose from the significant result of the group analysis from Experiment 2, because we could draw an inference from this result to the entire population of healthy young adult humans. This result from the group analysis did not address, however, an alternative model that posits comparable spatial and nonspatial working memory functions that are supported by topographically dissociable regions of the caudate nucleus [16]. This was because our group analysis technique, by collapsing across all voxels demonstrating delay-period activity, represented a ''winner-takes-all'' approach. We opted for this approach to maximize the sensitivity of our group analyses to experimentally induced changes in activation. Our single subject analyses, in contrast, were able to address the topographic-segregation-of-function hypothesis [16], because these included tests for main effects of stimulus material in delay-period activity, as well as for nonspatial delay-period activity that was dependent on impending motor contingencies. We did not find evidence to support the topographic segregation model of the functional organization of the caudate nucleus. This illustrates how the single-subject analyses and the group analyses described in this report were used to address different types of questions.

8. Essential literature references

Refs. [2,4,17,18,25–27]

Acknowledgements

Supported by the American Federation for Aging Research, and NIH grants NS01762 and AG13483. We thank Dustin Ballard, Jessica Lease, Rajiv Singh, and Elizabeth Wheeler for assistance with programming and data collection, and Geoffrey Aguirre for helpful discussions of this work.

References

[1] L. Abraham, M. Potegal, S. Miller, Evidence for caudate nucleus involvement in an egocentric spatial task: return from passive transport, Physiological Psychology 11 (1983) 11–17.
[2] G.K. Aguirre, M. D'Esposito, Experimental design for brain fMRI, in: C.T.W. Moonen, P.A. Bandettini (Eds.), Functional MRI, Springer Verlag, Berlin, 1999, pp. 369–380.
[3] G.K. Aguirre, E. Zarahn, M. D'Esposito, Empirical analyses of BOLD fMRI statistics: II. Spatially smoothed data collected under null-hypothesis and experimental conditions, NeuroImage 5 (1997) 199–212.
[4] G.K. Aguirre, E. Zarahn, M. D'Esposito, The variability of human, BOLD hemodynamic responses, NeuroImage 8 (1998) 360–369.
[5] J. Ashburner, K. Friston, Fully three-dimensional nonlinear spatial normalization: a new approach, NeuroImage 3 (1996) S111.
[6] D. Ballard, E. Zarahn, M. D'Esposito, Isolating the neural correlates of maintenance processes and motor set using event related fMRI. Journal of Cognitive Neuroscience, 1998 Annual Meeting Supplement (1998) 86.
[7] D. Cook, R.P. Kesner, Caudate nucleus and memory for egocentric localization, Behavioral and Neural Biology 49 (1988) 332–343.
[8] M. D'Esposito, B.R. Postle, D. Ballard, J. Lease, Maintenance versus manipulation of information held in working memory: an event-related fMRI study, Brain and Cognition 41 (1999) 66–86.
[9] M. D'Esposito, E. Zarahn, G.K. Aguirre, B. Rypma, The effect of normal aging on the coupling of neural activity to the BOLD hemodynamic response, NeuroImage 10 (1999) 6–14.
[10] K.J. Friston, J. Ashburner, C.D. Frith, J.-B. Poline, J.D. Heather, R.S.J. Frackowiak, Spatial registration and normalization of images, Human Brain Mapping 2 (1995) 165–189.
[11] K.J. Friston, A.P. Holmes, J.-B. Poline, J.D. Heather, R.S.J. Frackowiak, Analysis of fMRI time-series revisited, NeuroImage 2 (1995) 45–53.
[12] K.J. Friston, A.P. Holmes, K.J. Worsley, How many subjects constitute a study?, NeuroImage 10 (1999) 1–5.
[13] K.J. Friston, C.J. Price, P. Fletcher, C. Moore, R.S.J. Frackowiak, R.J. Dolan, The trouble with cognitive subtraction, NeuroImage 4 (1996) 97–104.
[14] O. Josephs, R. Turner, K. Friston, Event-related fMRI, Human Brain Mapping 5 (1997) 243–248.
[15] R. Kirk, Experimental Design: Procedures for the Behavioral Sciences, Brooks/Cole Publishing, Belmont, CA, 1982.
[16] R. Levy, H.R. Friedman, L. Davachi, P.S. Goldman-Rakic, Differential activation of the caudate nucleus in primates performing spatial and nonspatial working memory tasks, The Journal of Neuroscience 17 (1997) 3870–3882.
[17] B.R. Postle, M. D'Esposito, Dissociation of caudate nucleus activity

in spatial and nonspatial working memory: an event-related fMRI study, Cognitive Brain Research 8 (1999) 107–115.
[18] B.R. Postle, M. D'Esposito, ''What'' - then - ''where'' in visual working memory: an event-related fMRI study, Journal of Cognitive Neuroscience 11 (1999) 585–597.
[19] J. Quintana, J. Yajeya, J. Fuster, Prefrontal representation of stimulus attributes during delay tasks: I. Unit activity in cross-temporal integration of motor and sensory-motor information, Brain Research 474 (1988) 211–221.
[20] G. Rainer, S.C. Rao, E.K. Miller, Prospective coding for objects in the primate prefrontal cortex, Journal of Neuroscience 19 (1999) 5493–5505.
[21] S.C. Rao, G. Rainer, E.K. Miller, Integration of what and where in the primate prefrontal cortex, Science 276 (1997) 821–824.
[22] J. Talairach, P. Tournoux, Co-Planer Stereotaxic Atlas of the Human Brain, Thieme Medical Publishers, New York, 1988.
[23] M. Watanabe, Reward expectancy in primate prefrontal neurons, Nature 382 (1996) 629–632.
[24] R.P. Woods, Modeling for intergroup comparisons of imaging data, NeuroImage 4 (1996) S84–S94.
[25] K.J. Worsley, K.J. Friston, Analysis of fMRI time-series revisited-again, NeuroImage 2 (1995) 173–182.
[26] E. Zarahn, G.K. Aguirre, M. D'Esposito, Empirical analyses of BOLD fMRI statistics: I. Spatially unsmoothed data collected under null-hypothesis conditions, NeuroImage 5 (1997) 179–197.
[27] E. Zarahn, G.K. Aguirre, M. D'Esposito, A trial-based experimental design for fMRI, NeuroImage 6 (1997) 122–138.
[28] E. Zarahn, G.K. Aguirre, M. D'Esposito, Temporal isolation of the neural correlates of spatial mnemonic processing with functional MRI, Cognitive Brain Research 7 (1999) 255–268.